Physics Letters A 373 (2009) 964–968

Contents lists available at ScienceDirect

Physics Letters A

www.elsevier.com/locate/pla

# Stochastic resonance on Newman–Watts networks of Hodgkin–Huxley neurons with local periodic driving

Mahmut Ozer [a,*], Matjaž Perc [b], Muhammet Uzuntarla [a]

[a] Zonguldak Karaelmas University, Engineering Faculty, Department of Electrical and Electronics Engineering, 67100 Zonguldak, Turkey
[b] University of Maribor, Faculty of Natural Sciences and Mathematics, Department of Physics, Koroška cesta 160, SI-2000 Maribor, Slovenia

ARTICLE INFO

*Article history:*
Received 3 December 2008
Received in revised form 19 January 2009
Accepted 21 January 2009
Available online 24 January 2009
Communicated by R. Wu

*PACS:*
05.40.-a
87.16.-b
87.18.Sn
89.75.Hc

*Keywords:*
Stochastic process
Pacemaker
Small-world network
Neuronal dynamics

ABSTRACT

We study the phenomenon of stochastic resonance on Newman–Watts small-world networks consisting of biophysically realistic Hodgkin–Huxley neurons with a tunable intensity of intrinsic noise via voltage-gated ion channels embedded in neuronal membranes. Importantly thereby, the subthreshold periodic driving is introduced to a single neuron of the network, thus acting as a pacemaker trying to impose its rhythm on the whole ensemble. We show that there exists an optimal intensity of intrinsic ion channel noise by which the outreach of the pacemaker extends optimally across the whole network. This stochastic resonance phenomenon can be further amplified via fine-tuning of the small-world network structure, and depends significantly also on the coupling strength among neurons and the driving frequency of the pacemaker. In particular, we demonstrate that the noise-induced transmission of weak localized rhythmic activity peaks when the pacemaker frequency matches the intrinsic frequency of subthreshold oscillations. The implications of our findings for weak signal detection and information propagation across neural networks are discussed.



## 1. Introduction

The dynamics of complex networks has attracted much attention in recent years [1–4]. Two distinct types of topology; namely small-world (SW) [5] and scale-free (SF) networks [6], have been widely used due to their potential in capturing the characteristics of many real-world complex networks. Small-world networks have been suggested to provide a successful tool to search for connectivity information of both anatomical and functional networks in the brain, mainly because this topology can support both local and distributed information processing [7]. Functional connectivity is defined as temporal correlations between spatially distinct brain regions [8], and disturbances in the functional connectivity have been proposed as a major pathophysiological mechanism for cognitive disorganization [9]. Moreover, SW functional connectivity has been described in low and high frequency bands of healthy, resting-state magnetoencephalography (MEG) recordings [10]. Recent studies indicate a disrupted SW functional connectivity organization in schizophrenia [9,11]. The usefulness of SW measures has also been suggested for imaging-based biomarkers to distinguish between Alzheimer's disease and healthy aging [12].

It is also a central topic in theoretical and computational neuroscience to understand how neuronal circuitry generates complex patterns of activity. In this context, Lago-Fernandez et al. [13] showed that SW networks of Hodgkin–Huxley (HH) neurons have dynamic characteristics of both regular and random networks. Kwon and Moon [14] investigated the role of different connectivity regimes on the dynamics of HH neuronal networks, and found that increasing the network randomness may lead to an enhancement of temporal coherence and spatial synchronization of the network. In a recent study, we examined the noise-delayed decay (NDD) phenomenon on a small-world HH network [15]. Notably, the NDD is related to the noise-induced response delay with respect to the time of the first spike, whereby we showed that the network structure plays a key role only for intermediate coupling strengths where the NDD effect decrease, thus improving the signal detection rate.

Understanding the weak signal detection and information propagation in neuronal networks is of great importance. Noise can provide improvements in the representation of weak signals through stochastic resonance [16,17]. Gong et al. [18] studied the temporal coherence and spatial synchronization of HH neuronal networks subject to channel noise and subthreshold periodic stim-

* Corresponding author. Tel.: +90 372 257 5446; fax: +90 372 257 4023.
*E-mail address:* mahmutozer2002@yahoo.com (M. Ozer).

0375-9601/$ – see front matter 
doi:10.1016/j.physleta.2009.01.034

ulus, and found that the temporal coherence is maximal for an optimal fraction of randomly added shortcuts. We recently extended this study and showed that the collective temporal coherence peaks when the frequency of the subthreshold stimulus matches that of the intrinsic subthreshold oscillations for the HH neurons at a given fixed coupling strength and channel noise [19]. Wang et al. [20] also reported similar findings in a spatially extended network, which is locally modeled by a two-dimensional Rulkov map [21]. Furthermore, results in [19] also demonstrate a resonance-like effect depending on cell size, whereby an optimal size of cells leads to the maximum overall coherence in the system. Importantly, these studies consider the dynamics of neuronal networks on which every constitutive unit is subject to a weak periodic stimulus.

On the other hand, due to importance of pacemakers in real-life systems [22–25], it is also of great significance to introduce a weak periodic pacemaker to only a single element of the network and study the global outreach of the pacemaker. Therefore, the operation of the pacemakers has already been widely investigated in excitable systems [26–31], as well as in networks with complex connection topologies [32–37]. Our aim in this Letter is to extend the subject by including a more biophysically realistic model of individual neurons on the network, where the stochastic behavior of voltage-gated ion channels embedded in neuronal membranes is modeled depending on the cell size. This will allow relating the cell size (and thus the level of intrinsic noise) to the outreach of the pacemaker to other units of the network in a manner that more closely mimics actual conditions. Although we here use the same network model as in [19], we emphasize that there each neuron was subjected to a weak periodic driving, whereas presently only a single neuron is subjected to it, and thus the latter acts as a pacemaker on the network. Moreover, the measure for stochastic resonance employed presently is not just different from what was used in [19], but indeed quantifies a different phenomenon. Note that in [19] only the temporal coherence has been studied, whereas here we focus explicitly on the stochastic resonance; that is the presence of a given frequency (not just any frequency as in temporal coherence) in the output of each neuron. In what follows, we investigate the global outreach of the pacemaker as a function of the cell size (thus, ion channel noise), coupling strength as well as pacemaker frequency and network topology.

## 2. Model and methods

The time evolution of the membrane potential for coupled HH neurons on a network is given by [18,19]:

$$C_m \frac{dV_i}{dt} = -g_{\mathrm{Na}} m_i^3 h_i (V_i - V_{\mathrm{Na}}) - g_{\mathrm{K}} n_i^4 (V_i - V_{\mathrm{K}}) - g_L (V_i - V_L) + \sum_j \varepsilon_{ij} (V_j - V_i), \quad (1)$$

where $V_i$ denotes the membrane potential of neuron $i = 1, 2, \ldots, N$ ($N$ being the system size), $C_m = 1\ \mu\mathrm{F\,cm^{-2}}$ is the membrane capacity, whereas $g_{\mathrm{Na}} = 120\ \mathrm{mS\,cm^{-2}}$ and $g_{\mathrm{K}} = 36\ \mathrm{mS\,cm^{-2}}$ are the maximal sodium and potassium conductance, respectively. The leakage conductance is assumed to be constant, equaling $g_L = 0.3\ \mathrm{mS\,cm^{-2}}$, and $V_{\mathrm{Na}} = 50$ mV, $V_{\mathrm{K}} = -77$ mV and $V_L = -54.4$ mV are the reversal potentials for the sodium, potassium and leakage channels, respectively. Moreover, $\varepsilon_{ij}$ denotes the coupling strength between neurons $i$ and $j$, whereby we set $\varepsilon_{ij} = \varepsilon$ if the two are connected or $\varepsilon_{ij} = 0$ otherwise. Finally, $m_i$ and $h_i$ denote activation and inactivation variables for the sodium channel of neuron $i$, respectively, and the potassium channel includes an activation variable $n_i$.

In the HH model, activation and inactivation gating variables $m_i$, $n_i$ and $h_i$ change over time in response to the membrane potential following first-order differential equations within the limit of a very large cell size [38]. However, when the population of ion channels is finite, the stochastic dynamics of voltage-gated ion channels (or ion channel noise) can have significant implications on the excitable behavior of neurons [39–44]. The effects of the channel noise can be modeled with different computational algorithms [45]. In this study, we use the algorithm presented by Fox [46], both because it is widely used [19,44,47–52] and because other algorithms can be very time-consuming, especially for larger cell sizes. In the Fox's algorithm, variables of stochastic gating dynamics are described via the Langevin generalization [46]:

$$\frac{dx_i}{dt} = \alpha_x (1 - x_i) - \beta_x x_i + \xi_{x_i}(t), \quad x_i = m_i, n_i, h_i, \quad (2)$$

where $\alpha_x$ and $\beta_x$ are rate functions for the gating variable $x_i$. The probabilistic nature of the channels appears as a source of noise $\xi_{x_i}(t)$ in Eq. (2), which is an independent zero mean Gaussian white noise whose autocorrelation function is given by [27]:

$$\langle \xi_m(t) \xi_m(t') \rangle = \frac{2\alpha_m \beta_m}{N_{\mathrm{Na}}(\alpha_m + \beta_m)} \delta(t - t'), \quad (3)$$

$$\langle \xi_h(t) \xi_h(t') \rangle = \frac{2\alpha_h \beta_h}{N_{\mathrm{Na}}(\alpha_h + \beta_h)} \delta(t - t'), \quad (4)$$

$$\langle \xi_n(t) \xi_n(t') \rangle = \frac{2\alpha_n \beta_n}{N_{\mathrm{K}}(\alpha_n + \beta_n)} \delta(t - t'), \quad (5)$$

where $N_{\mathrm{Na}}$ and $N_{\mathrm{K}}$ denote the total number of sodium and potassium channels, respectively. The channel numbers are calculated as $N_{\mathrm{Na}} = \rho_{\mathrm{Na}} S$ and $N_{\mathrm{K}} = \rho_{\mathrm{K}} S$, where $\rho_{\mathrm{Na}} = 60\ \mu\mathrm{m^{-2}}$ and $\rho_{\mathrm{K}} = 18\ \mu\mathrm{m^{-2}}$ are the sodium and potassium channel densities, respectively, whereas $S$ is the membrane cell area. Eqs. (1)–(5) constitute the stochastic HH network model, where the cell size $S$ determines the intensity of intrinsic noise. When the cell size is large enough, stochastic effects of the channel noise are negligible, and thus the stochastic model approaches the deterministic description.

The network is comprised of identical coupled HH neurons, initially each having connectivity $k = 2$, with the system size set to $N = 60$. Following the Newman–Watts model [53], we start with a regular ring and make a random draw of two neurons. Subsequently, if they are not already connected, we add a non-directed link between them. This process is repeated until a total of $M$ new links have been added, finally resulting in an equivalent network of adding new edges with a probability $p$, which is given by [15,18,19]:

$$p = \frac{2M}{N(N-1)}. \quad (6)$$

Localized weak rhythmic activity is introduced in form of a subthreshold pacemaker of the form $I_r(t) = A \sin(\omega t)$, which is added additively to the middle neuron $i = r = 30$ in Eq. (1). Here $A$ denotes the amplitude of the sinusoidal forcing current, which we set to 1.0 $\mu\mathrm{A/cm^2}$, whereas $\omega$ is the corresponding angular frequency. Notably, since the degree heterogeneity of small-world networks follows a Poissonian distribution in the $p \to 1$ limit, the particular placing of the pacemaker within the network is not of vital importance [37].

For each set of $\varepsilon, p, S$ and $\omega$ the temporal output of each neuron given by $V_i(t)$ is recorded for $T = 1000$ periods of the pacemaker, and then the collective temporal behavior of the network is measured by calculating the average membrane potential $V_{\mathrm{avg}}(t) = N^{-1} \sum_{i=1,\ldots,N} V_i(t)$ corresponding to the mean field of a random network. The correlation of each series with the frequency of the pacemaker $\omega = 2\pi/t_r$ is computed via the Fourier coefficients $Q = \sqrt{R^2 + S^2}$ according to [54]:

$$R = \frac{2}{Tt_r}\int_0^{t_r T} V_{\mathrm{avg}}(t)\sin(\omega t)\,dt, \tag{7}$$

$$S = \frac{2}{Tt_r}\int_0^{t_r T} V_{\mathrm{avg}}(t)\cos(\omega t)\,dt. \tag{8}$$

Since the Fourier coefficients are proportional to the square of the spectral power amplification [55], we presently use $Q$ as the measure for stochastic resonance. In addition, we also evaluate $Q_i$ separately for each neuron, whereby $V_{\mathrm{avg}}(t)$ in Eqs. (7) and (8) is replaced by $V_i(t)$. Below presented results were obtained by averaging $Q$ and $Q_i$ over 50 different realizations of the underlying network structure for each $p$.

## 3. Results and discussion

In what follows, we will systemically analyze effects of different $\varepsilon$, $p$, $S$ and $\omega$ on the transmission of localized rhythmic activity via $Q$ and $Q_i$. First, we examine the dependence of $Q_i$ on $S$ and $i$ for different $p$ with fixed values for the coupling strength ($\varepsilon = 0.05$) and the angular frequency of the pacemaker ($\omega = 0.3$ ms$^{-1}$). Fig. 1 features the resulting color-contour plots for increasing values of $p$ from top to bottom. It is evident that there exists an optimal cell size by which $Q_i$ across the whole network are maximal, indicating the existence of pacemaker-driven stochastic resonance. It can also be inferred that the optimal outreach of the localized rhythmic activity across all neurons is warranted by $p = 0.1$, indicating the ability of fine-tuning of the network structure via $p$ to optimize the phenomenon of stochastic resonance.

To gain more insights into the dependence of the outreach of the pacemaker on $\varepsilon$ and $p$, we calculate the dependence of $Q$ on $p$ by three different coupling strengths $\varepsilon$, with a fixed cell size $S = 6$ μm$^2$. Results are presented in Fig. 2. Evidently, $Q$ exhibits a resonance-like behavior with respect to $p$ at the fixed value of the channel noise strength, thus indicating the existence of an optimal small-world topology for the transmission of localized rhythmic activity. Notably, similar results were recently obtained for a noisy array of overdamped bistable oscillators [37]. At the fixed value of the channel noise strength equaling $S = 6$ μm$^2$, we found that the value of $p$ which gives the maximal $Q$ decreases when the coupling strength increases. Thus, as the coupling increases the peak $Q$ is obtained for fewer added shortcuts, or equivalently, by a lower value of $p$. This finding is consistent with our previous results [19], although the latter were related to the collective temporal regularity whereby we used the same network model. Wang et al. [56] also found that the optimal $p$ value for the temporal coherence of the system decreases when the coupling strength is increased by using the same network topology. Although Perc [35] found that there exists an optimal value of the coupling strength for which the network structure plays a key role for the transmission of localized rhythmic activity by using the Watts–Strogatz network model based on the Rulkov map [21], the currently investigated network model does not reveal such a property for the transmission of localized rhythmic activity. The qualitative difference may be a consequence of the different initial connectivity of neurons ($k = 6$ in [21]), or the different scaling of the clustering coefficient in dependence on $p$ for the Watts–Strogatz and the presently used small-world topology. Moreover, we found that the maximal $Q$ decreases as the coupling strength increases (see Fig. 2), which however, is consistent with the results by Perc and Gosak [37] for a diffusive network (see their Fig. 4). On the other hand, stronger coupling strength contributes to a higher value of $Q$ in regular network (in the limit $p \to 0$).

Next, we present the dependence of $Q_{i=30}$ and $Q$ on the ion channel noise strength $S$ for a fixed value of the coupling strength

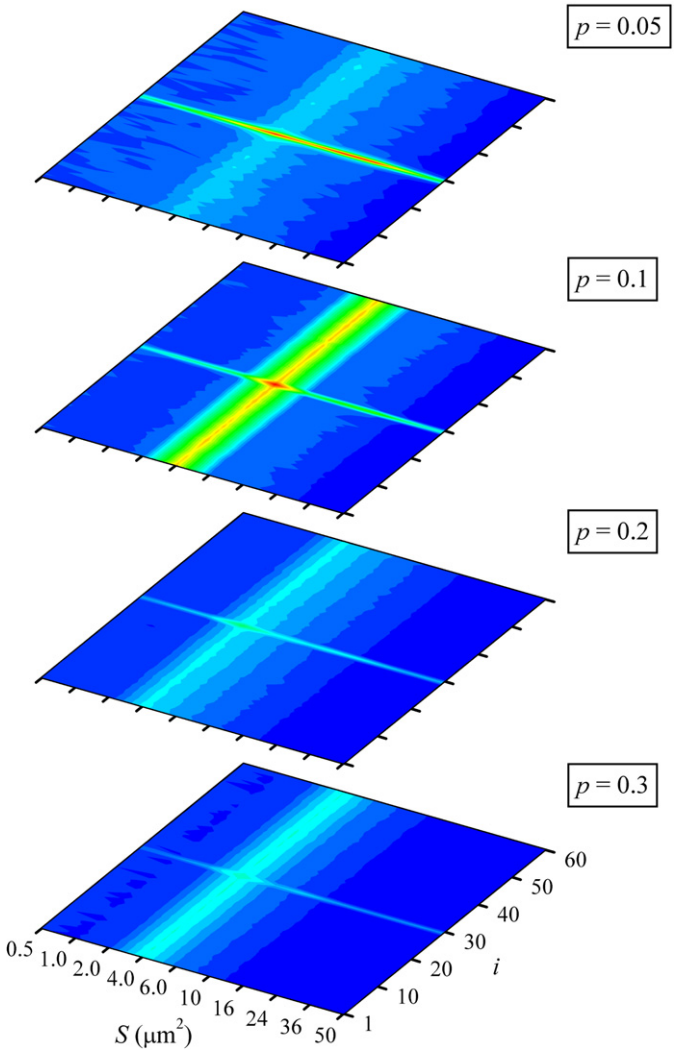


**Fig. 1.** Color-coded $Q_i$ in dependence on $S$ and $i$ for different $p$ and a fixed coupling strength $\varepsilon = 0.05$. In all panels the pacemaker has been introduced to the middle oscillator $i = r = 30$ and the color profile is linear, blue marking minimal and red maximal values of $Q_i$. The intervals of $Q_i$ are the same in all panels, spanning from $Q_i = 0.0$ (blue) to $Q_i = 4.5$ (red). Note that the overall maximum of $Q_i$ (obtained by $i = r = 30$) decreases continuously as $p$ increases, yet the optimal outreach across all units is warranted by $p = 0.1$. (For interpretation of the references to color in this figure legend, the reader is referred to the web version of this Letter.)

($\varepsilon = 0.05$) by different $p$ in Fig. 3. Results for both the collective network behavior ($Q$) and the pacemaker-driven neuron ($Q_{i=30}$) indicate that there exists a certain range of $S$ values for each particular $p$, by which the corresponding intrinsic noise is able to optimally assist the pacemaker in driving the neuronal network. In particular, as $p$ increases the peaks of $Q_{i=30}$ and $Q$ are obtained for slightly smaller patch areas, i.e. larger noise intensities (Fig. 3). Since the pacemaker-driven neuron exhibits the most correlated response with respect to the subthreshold periodic forcing, its maximal $Q_{i=30}$ is larger than that for the rest of the network [37]. The optimal noise level corresponds to a cell size of around 4–6 μm$^2$ regardless of the position of the neuron within the network, or the consideration of the collective network response or the response of solely the pacemaker-driven neuron. Although presently only a single neuron is subjected to the weak periodic driving, this finding is also consistent with our previous work [19] (there every neuron was subjected to the driving) where the optimal noise level for the collective temporal coherence of an identical neuronal network was found to equal around 4–6 μm$^2$.

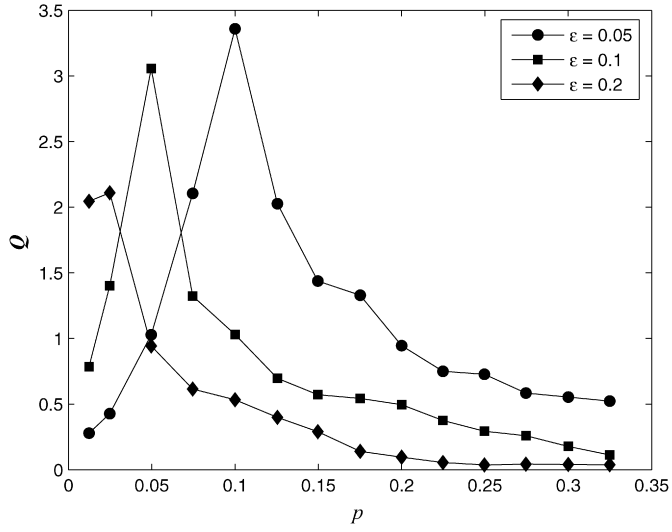


**Fig. 2.** The dependence of $Q$ on $p$ for three different coupling strengths $\varepsilon$, obtained by a fixed patch area equaling $S = 6\ \mu m^2$.

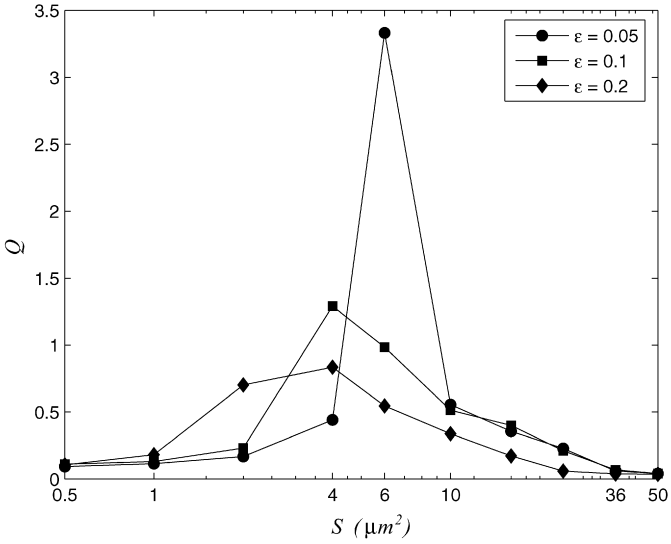


**Fig. 4.** The dependence of $Q$ on $S$ for three different coupling strengths $\varepsilon$, obtained by $p = 0.1$.

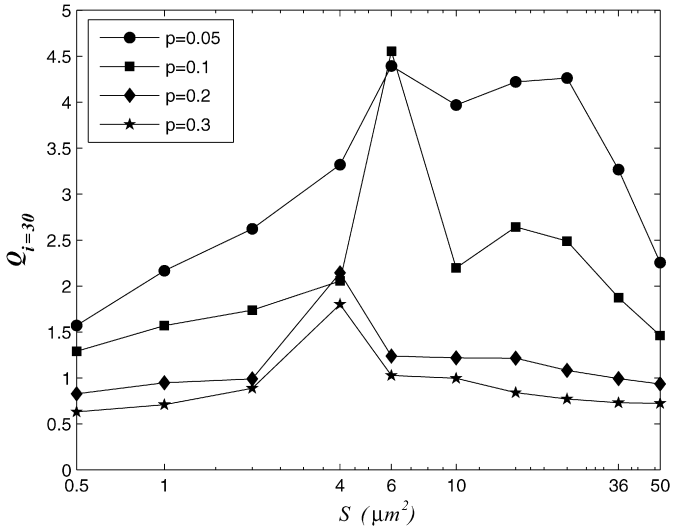


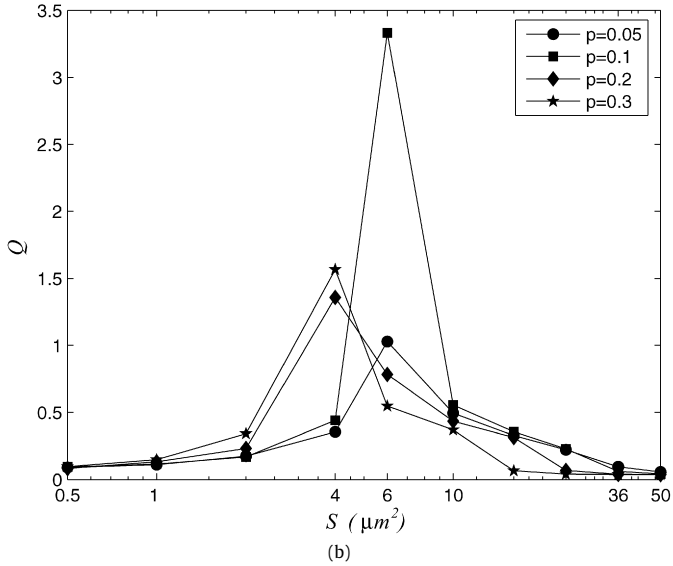


**Fig. 3.** The dependence of $Q_{i=30}$ [panel (a)] and $Q$ [panel (b)] on the patch area $S$ for four different values of $p$, obtained by a fixed coupling strength $\varepsilon = 0.05$.

Importantly, however, the maximal $Q$ is obtained when both the cell size and the fraction of random shortcuts have optimal values ($S = 6\ \mu m^2$, $p = 0.1$). Therefore, we further investigate how the maximal $Q$ changes with the coupling strength and cell size when $p$ is equal to 0.1. Obtained results of this analysis are presented in Fig. 4. Evidently, the maximal $Q$ decreases with increasing $\varepsilon$, and at the same time smaller and smaller cell sizes are needed to evoke the optimal response. This is in agreement with the results by Perc and Gosak [37], who also reported that the optimal noise strength increases continuously with increasing $\varepsilon$ (and accordingly the maximally attainable $Q_i$ decrease), although the latter result was obtained only for a pacemaker-driven network of overdamped oscillators, but not for a realistic neuron model.

Thus far, the pacemaker frequency was chosen equal to $\omega = 0.3\ ms^{-1}$ (or $f \approx 50$ Hz), corresponding to the frequency of intrinsic subthreshold oscillations of HH neurons [57]. Due to the importance of frequency tuning in weak signal detection and transmission [17,57–60], we investigate the impact of different driving frequencies on the global outreach of the pacemaker. We calculate the dependence of $Q$ on $p$ by different pacemaker frequencies $\omega$ with fixed values for the coupling strength ($\varepsilon = 0.05$) and cell size ($S = 6\ \mu m^2$). Fig. 5 features obtained results. It can be observed that $Q$ exhibits a resonance-like behavior with respect to $p$ only for $\omega = 0.3\ ms^{-1}, \omega = 0.6\ ms^{-1}$ and $\omega = 0.9\ ms^{-1}$, but not for other values of the driving frequency. Notably though, the second and third harmonics of the intrinsic oscillations, given by $\omega = 0.6\ ms^{-1}$ and $\omega = 0.9\ ms^{-1}$, already results in a substantially lower peak of $Q$. Moreover, values of $Q$ for driving frequencies that are different from the intrinsic HH frequency, or their higher harmonics, are virtually independent of the network topology. Thus, we conclude that the global outreach of the pacemaker peaks when the pacemaker frequency matches that of the intrinsic subthreshold oscillations of the individual network elements. In a recent study we showed that the collective temporal coherence of a stochastic small-world HH neuronal network, which is globally driven by a weak periodic driving, also peaks when the frequency of the external stimulus matches the intrinsic frequency of constitutive units of the network [19]. Both results therefore suggest that the network rhythmicity reflects a direct coupling between oscillatory properties of individual network elements [61,62]. Our results also answer in part the question, as to what extent the pacemaker is able to induce a synchronous response of the network with a frequency different from the intrinsic noise-induced one [30].

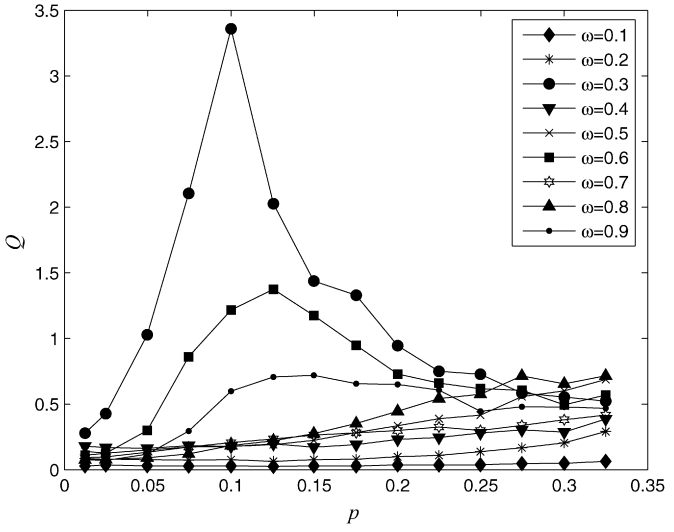


**Fig. 5.** The dependence of $Q$ on $p$ for nine different values of $\omega$, obtained by a fixed patch area $S = 6\ \mu m^2$ and coupling strength $\varepsilon = 0.05$.

The study of pacemaker activity is vital for several biological systems, and thus it certainly deserves separate attention. Probably the most prominent organ that has pacemaker cells is the human heart [63]; but also many arteries and arterioles, exhibit localized rhythmical contractions that are synchronous over considerable distances [64]. A well-known network of pacemaker cells are also the so-called interstitial cells of Cajal (ICC), which regulate the contractility of many smooth muscle cells in several organs, particularly in the gastrointestinal tract [65] and the urethra [66]. Recently, non-contractile cells closely resembling ICC were identified also in the wall of portal veins and mesenteric arteries [67]. Moreover, it should be noted that pacemakers are not characteristic only for whole organs or tissue, but may also be encountered in larger cells like eggs, where cortical endoplasmic reticulum rich clusters act as pacemaker sites dedicated to the initiation of global calcium waves which then propagate throughout the egg [68]. In this context, we hope this study will spawn new research related to the noise-supported detection and transmission of weak localized rhythmic activity across complex networks.

## Acknowledgement

Matjaž Perc acknowledges support from the Slovenian Research Agency (grant Z1-9629).

## References

[1] S. Lawrence, C.L. Giles, Science 280 (1998) 98.
[2] R. Albert, H. Jeong, A.-L. Barabasi, Nature 401 (1999) 130.
[3] M.E.J. Newman, Proc. Natl. Acad. Sci. USA 98 (2001) 404.
[4] S.H. Strogatz, Nature 410 (2001) 268.
[5] D.J. Watts, S.H. Strogatz, Nature 393 (1998) 440.
[6] A.-L. Barabasi, R. Albert, Science 286 (1999) 509.
[7] D.S. Basset, E. Bullmore, The Neuroscientist 12 (2006) 512.
[8] K.J. Friston, C.D. Frith, P.F. Liddle, R.S. Frackowiak, J. Cereb, Blood Flow Metab. 13 (1993) 5.
[9] S. Micheloyannis, E. Pachou, C.J. Stam, M. Breakspear, P. Bitsios, M. Vourkas, S. Erimaki, M. Zerkavis, Schizophr. Res. 87 (2006) 60.
[10] C.J. Stam, J. Neurosci. Lett. 355 (2004) 25.
[11] Y. Liu, M. Liang, Y. Zhou, Y. He, Y. Hao, M. Song, C. Yu, H. Liu, Z. Liu, T. Jiang, Brain 131 (2008) 945.
[12] K. Supekar, V. Menon, D. Rubin, M. Musen, M.D. Greicius, PLoS Comput. Biol. 4 (2008) e1000100.
[13] L.F. Lago-Fernandez, R. Huerta, F. Corbacho, J.A. Siguenza, Phys. Rev. Lett. 84 (2000) 2758.
[14] O. Kwon, H.T. Moon, Phys. Lett. A 298 (2002) 319.
[15] M. Ozer, M. Uzuntarla, Phys. Lett. A 372 (2008) 4603.
[16] S.M. Bezrukov, I. Vodyanov, Nature 378 (1995) 362.
[17] J.E. Levin, J.P. Miller, Nature 380 (1996) 165.
[18] Y. Gong, M. Wang, Z. Zhou, H. Xin, Chem. Phys. Chem. 6 (2005) 1042.
[19] M. Ozer, M. Uzuntarla, T. Kayikcioglu, L.J. Graham, Phys. Lett. A 372 (2008) 6498.
[20] Q.Y. Wang, Q.S. Lu, G.R. Chen, Europhys. Lett. 77 (2007) 10004.
[21] N.F. Rulkov, Phys. Rev. Lett. 86 (2001) 183.
[22] K.J. Lee, E.C. Cox, R.E. Goldstein, Phys. Rev. Lett. 76 (1996) 1174.
[23] B. Blasius, A. Huppert, L. Stone, Nature 399 (1999) 354.
[24] J.J. Toyson, P.C. Fife, J. Chem. Phys. 73 (1980) 2224.
[25] M. Stich, M. Ipsen, A.S. Mikhailov, Phys. Rev. Lett. 86 (2001) 4406.
[26] Y. Nagai, H. Gonzales, A. Shrier, L. Glass, Phys. Rev. Lett. 84 (2000) 4248.
[27] S. Alonso, I. Sendina-Nadal, V. Perez-Munuzuri, J.M. Sancho, F. Sagues, Phys. Rev. Lett. 87 (2001) 078302.
[28] M. Gutman, I. Aviram, A. Rabinovitch, Phys. Rev. E 70 (2004) 037202.
[29] V. Jacquement, Phys. Rev. E 74 (2006) 011908.
[30] M. Perch, M. Marhi, Phys. Lett. A 353 (2006) 372.
[31] T.R. Chigwada, P. Parmananda, K. Showalter, Phys. Rev. Lett. 96 (2006) 244101.
[32] H. Kori, A.S. Mikhailov, Phys. Rev. Lett. 93 (2004) 254101.
[33] F. Radicchi, H. Meyer-Ortmanns, Phys. Rev. E 73 (2006) 036218.
[34] A.J. Steele, M. Tinsley, K. Showalter, Chaos 16 (2006) 015110.
[35] M. Perc, Phys. Rev. E 76 (2007) 066203.
[36] M. Perc, Phys. Rev. E 78 (2008) 036105.
[37] M. Perc, M. Gosak, New J. Phys. 10 (2008) 053008.
[38] A.L. Hodgkin, A.F. Huxley, J. Physiol. (London) 117 (1952) 500.
[39] E. Skaugen, L. Walloe, Acta Physiol. Scand. 107 (1979) 343.
[40] J.T. Rubinstein, Biophys. J. 68 (1995) 779.
[41] C.C. Chow, J.A. White, Biophys. J. 71 (1996) 3013.
[42] E. Schneidman, B. Freedman, I. Segev, Neural Comput. 10 (1998) 1679.
[43] J.A. White, J.T. Rubinstein, A.R. Kay, Trends Neurosci. 23 (2000) 131.
[44] M. Ozer, N.H. Ekmekci, Phys. Lett. A 338 (2005) 150.
[45] H. Mino, J.T. Rubinstein, J.A. White, Ann. Biomed. Eng. 30 (2002) 578.
[46] R.F. Fox, Biophys. J. 72 (1997) 2069.
[47] G. Schmid, I. Goychuk, P. Hänggi, Europhys. Lett. 56 (2001) 22.
[48] G. Schmid, I. Goychuk, P. Hänggi, Physica A 325 (2003) 165.
[49] G. Schmid, I. Goychuk, P. Hänggi, Phys. Biol. 1 (2004) 61.
[50] M. Ozer, Phys. Lett. A 354 (2006) 258.
[51] M. Ozer, M. Uzuntarla, S.N. Agaoglu, Phys. Lett. A 360 (2006) 135.
[52] G. Schmid, P. Hänggi, Math. Biosci. 207 (2007) 235.
[53] M.E.J. Newman, D.J. Watts, Phys. Lett. A 263 (1999) 341.
[54] W.H. Press, S.A. Teukolsky, W.T. Vetterling, B.P. Flannery, Numerical Recipes in C, Cambridge Univ. Press, Cambridge, 1995.
[55] L. Holden, T. Erneux, SIAM J. Appl. Math. 53 (1993) 1045.
[56] M. Wang, Z. Hou, H. Xin, Chem. Phys. Chem. 7 (2006) 579.
[57] Y. Yu, W. Wang, J.F. Wang, F. Liu, Phys. Rev. E 63 (2001) 021907.
[58] W. Wang, Y. Wang, Z.D. Wang, Phys. Rev. E 57 (1998) 2527.
[59] F. Liu, J.F. Wang, W. Wang, Phys. Rev. E 59 (1999) 3453.
[60] F. Liu, J.F. Wang, W. Wang, Phys. Lett. A 256 (1999) 181.
[61] R.R. Llinas, Science 242 (1998) 1654.
[62] B. Hutcheon, Y. Yarom, Trends Neurosci. 23 (2000) 216.
[63] A.M. Katz, Physiology of the Heart, Kluwer, Philadelphia, 2000.
[64] R.E. Haddock, C.E. Hill, J. Physiol. 566 (2005) 645.
[65] K.M. Sanders, T. Ördög, S.D. Koh, S.M. Ward, News Physiol. Sci. 15 (2000) 291.
[66] G.D.S. Hirst, S.M. Ward, J. Physiol. 550 (2003) 337.
[67] T.B. Bolton, D.V. Gordienko, O.V. Povstyan, M.I. Harhun, V. Pucovsky, Cell Calcium 35 (2004) 643.
[68] R. Dumollard, J. Caroll, G. Dupont, C. Sardet, J. Cell. Sci. 115 (2002) 3557.